



Inverse-catalyst-effect observed for nanocrystalline-doped tin oxide sensor at lower operating temperatures

S. Shukla^a, L. Ludwig^b, C. Parrish^b, S. Seal^{a,*}

^a Surface Engineering and Nanotechnology Facility, Mechanical Materials Aerospace Engineering (MMAE) Department and Advanced Materials Processing and Analysis Center (AMPAC), University of Central Florida (UCF), Engineering #381, 4000 Central Florida Blvd., Orlando, FL 32826, USA

^b Kennedy Space Center, KSC (NASA), Orlando, FL 32899, USA

Received 3 December 2003; received in revised form 26 April 2004; accepted 12 May 2004

Abstract

Nanocrystalline In_2O_3 -doped SnO_2 thin film sensor is synthesized via sol–gel dip-coating technique. This nanocrystalline thin film is successfully utilized to sense hydrogen (H_2) gas with the concentration as low as 50 ppm at lower operating temperatures (25–100 °C). For short test-duration (30 min), the H_2 sensitivity of the Pt-sputtered sensor is observed to be higher than that of the non-Pt-sputtered film. An “inverse-catalyst-effect” on the H_2 gas sensitivity is, however, newly observed when the test-duration is increased to 24 h. The presence of H_2O molecules, which remain adsorbed and get accumulated on the sensor surface, during the long test-duration, are primarily attributed to the reduced H_2 gas sensitivity of the Pt-sputtered sensors, relative to that of non-Pt-sputtered sensors, at lower operating temperatures (25–100 °C).

© 2004 Elsevier B.V. All rights reserved.

Keywords: Hydrogen; Indium oxide; Inverse-catalyst-effect; Lower operating temperatures; Sensor; Sol–gel; Thin films; Tin oxide

1. Introduction

Nanocrystalline tin oxide (SnO_2) thin film is a well-known n-type semiconductor gas sensor [1]. It is now recognized that the sensitivity of SnO_2 sensor can be enhanced drastically by reducing the nanocrystallite size below 10 nm due to the enhancement in the receptor and the transducer functions of the sensor below this critical size range [2–5]. Moreover, the gas sensitivity of the nanocrystalline SnO_2 sensor is reported to be maximum for the film thickness of 70–100 nm [6,7] and within the operating temperature range of 350–450 °C; above and below which the gas sensitivity decreases [8]. Use of trivalent dopants, which enhances the space-charge-layer thickness via generation of lattice oxygen-ion vacancies, has been traditional approach to enhance the gas sensitivity of nanocrystalline SnO_2 sensor [4]. The presence of surface-catalyst and the surface foreign oxides are also known to enhance the gas sensitivity of nanocrystalline SnO_2 sensor [2,4,9–12].

Thus, the gas sensing characteristics of nanocrystalline SnO_2 sensor appears to be well established. However, the literature indicates that the most of the research conducted till now has been concentrated in the high temperature region (>100 °C) and very less or no attention has been paid in the low temperature (<100 °C) range. Most of the industrial applications, however, demand the gas sensors to be operated at lower temperatures (especially at room temperature) to avoid the instability in the nanocrystallite size, and hence, to increase the robustness and the life of the sensor. In spite of the awareness of these conditions, no attempt is being made to develop the nanocrystalline SnO_2 sensors operating at lower temperatures. Very low gas sensitivity, and very high response and recovery time, at lower operating temperatures are the major issues, which are yet to be resolved in the lower operating temperature range. Moreover, the role of a surface catalyst at lower operating temperatures is not yet precisely understood. It will be shown in the present article that, although the surface-catalyst enhances the gas sensitivity at higher temperatures, it may have an adverse effect at lower operating temperatures. Such a study is, however, lacking in the present literature. From this point of view, the objectives of the present article are set to demonstrate the

* Corresponding author. Tel.: +1 407 882 1184; fax: +1 407 823 0208.
E-mail address: sshukla@pegasus.cc.ucf.edu (S. Seal).

sensing of H₂ gas with the concentration as low as 50 ppm at lower operating temperatures (<100 °C); and secondly, to discuss an “inverse-catalyst-effect” (a new finding) typically observed for the Pt-sputtered nanocrystalline SnO₂ sensor.

2. Experimental

2.1. Materials

Tin(IV)-isopropoxide (Sn[OC₃H₇]₄) (10 w/v%) in *iso*-propanol (72 vol.%) and toluene (18 vol.%) and indium(III)-isopropoxide (In[OC₃H₇]₃) were purchased from Alfa Aesar (USA) and used as received. Small glass substrates (1 cm × 1 cm) were cut from the Pyrex glass slides, which were received from the Fisher Scientific (USA), for the dip-coating experiments.

2.2. Processing of nanocrystalline indium oxide (In₂O₃)-doped SnO₂ thin films

Indium oxide (In₂O₃)-doped SnO₂ thin films coated on the Pyrex glass (silica) substrates were processed via sol-gel dip-coating technique. The glass substrates were ultrasonically cleaned, first in acetone and then in *iso*-propanol. The pre-cleaned substrates were dipped in the solution of tin-isopropoxide in *iso*-propanol and toluene, corresponding to the concentration of 0.23 M of tin-isopropoxide, using a dip-coater and withdrew with a speed of 150 cm/min. Calculated amount of indium(III)-isopropoxide was dissolved in this solution to obtain thin films of SnO₂-6.5 mol% In₂O₃. After the dip-coating process, the gel films were dried at 150 °C for 1 h in air. The substrates were dip-coated again under similar conditions and then dried again at 150 °C for 1 h in air. Some of the dried gel films were sputtered with a thin (3–5 nm) layer of Pt for 10 s using a sputter coater (K350, Emitech Ltd., Ashford, Kent, UK). Finally, Pt-sputtered and non-Pt-sputtered dried films were fired at 500 and 600 °C in air. The samples were heated at a rate of 30 °C/min up to the firing temperature, held at that temperature for 1 h, and then cooled to room temperature inside the furnace. As demonstrated earlier [13], the present procedure results in the synthesis of SnO₂ thin films having thickness 100–150 nm with the nanocrystallite size of 6–8 nm.

2.3. Sensor test

The sensor-test set-up has already been described elsewhere [13]. The procedure used for the sensor-test is as follows. Four different thin film sensors (calcined at 500 and 600 °C, with and without Pt-sputtering) and one bare glass substrate (reference) were mounted on the software designed fiber glass test-board, which incorporated the heater, electrical, and thermocouple connections. During the testing, each sensor was connected in parallel with 10 MΩ resistance using a switcher circuit. The four-probe technique, with a

constant-current (100 nA) source, was used to measure the equivalent resistance (R_{eq}) in air as well as in the hydrogen-containing environment. The true resistance values for the thin film sensors in air (R_{air}) and in the hydrogen-containing environment (R_{gas}) were back calculated using the respective measured R_{eq} values. The hydrogen gas sensitivity was then determined using the relationship of the form:

$$\% \text{ Sensitivity} = \frac{R_{air} - R_{gas}}{R_{gas}} \times 100 \quad (1)$$

The sensor-test was first conducted at room temperature (25 °C). At the beginning of the test, pure-nitrogen gas was blown into the test-chamber, housing the test-board at 20 Torr, for 24 h to remove the water vapor and any residual hydrogen. The synthetic air was then purged into the chamber for the next 24 h to stabilize the sensor resistance, which was followed by the measurement of R_{air} values. A mixture of N₂ and H₂ gas (50 ppm of H₂ with respect to the chamber volume) was then admitted continuously, using the mass flow controllers, into the test-chamber containing air at 20 Torr. R_{gas} values were recorded after every 50 s for 24 h test-duration. At the end of the test, the air at 760 Torr was blown into the chamber to recover the initial resistance values of the sensors. Similar test procedure was then repeated by increasing the test-temperature to 50, 75, and 100 °C in steps.

Typical cyclic test, consisting of three cycles, was conducted for 50 ppm of H₂ (with respect to the chamber volume) at 75 °C. During this test, after stabilizing the sensor resistances in air at 20 Torr, the mixture of N₂ and H₂ gas was admitted into the chamber only for 30 min. Then, the flow of synthetic air was established till the original resistance values of the sensors were recovered. The entire test-cycle was then repeated two more times and, at the end, air at 760 Torr was blown into the chamber.

3. Results

Typical cyclic response of In₂O₃-doped SnO₂ sensors, one calcined at 500 °C with Pt and other calcined at 600 °C without Pt, for 50 ppm hydrogen, is presented in Fig. 1(a) and (b), respectively. The sensitivity values and recovery time recorded for the constant response time (test-duration) of 30 min for all four sensors, are tabulated in Table 1.

Table 1
Sensitivity and recovery time, recorded for the nanocrystalline In₂O₃-doped SnO₂ sensor under four different conditions, for the constant response time of 30 min at 75 °C

Sensor type	Response time (min)	Sensitivity (%)	Recovery time (min)
500-Pt	30	13	60
500	30	6	50
600-Pt	30	12	95
600	30	10	75

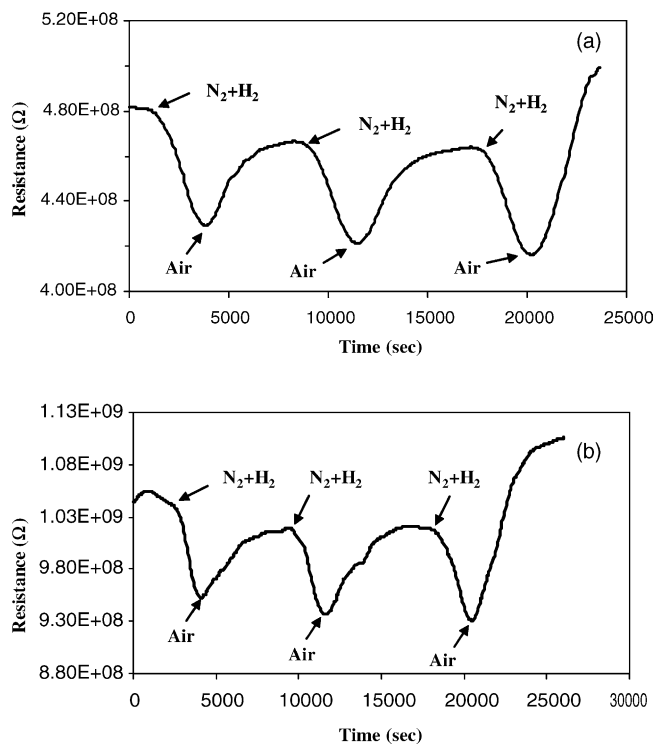


Fig. 1. Typical cyclic response of In_2O_3 -doped SnO_2 sensor at 75°C . The response time is kept constant to 30 min: (a) sensor calcined at 600°C with Pt-catalyst and (b) sensor calcined at 500°C without Pt-catalyst.

It is noted that the Pt-sputtered sensors show maximum sensitivity than the non-Pt-sputtered thin films. Moreover, the recovery time of the Pt-sputtered sensors is also larger relative to that for the non-Pt-sputtered sensors. In the case of Pt-sputtered sensors, the sensitivity is observed to be slightly higher for the sensor calcined at lower operating temperature; although this behavior is not observed for the non-Pt-sputtered sensors.

Typical response of In_2O_3 -doped SnO_2 sensors calcined at 500 and 600°C with Pt-sputtering, recorded for 50 ppm of hydrogen at 20 Torr air pressure, for the total test-duration of approximately 24 h, is presented in Figs. 2 and 3. Typical response behavior observed for one cycle at four different temperatures, within the range of 25 – 100°C , is presented in these figures. For the sensor calcined at 500°C with Pt-sputtering, the introduction of 50 ppm H_2 at 25°C , Fig. 2(a), results in a gradual decrease in the sensor resistance. However, the decrease in the sensor resistance is followed by an increase in the sensor resistance, in the presence of H_2 . The sensor resistance reaches its original value and begins to decrease again. The original sensor resistance is, however, again retained by purging air at 20 and 760 Torr in sequence. The increase in the sensor resistance after its initial drop is systematically observed at 50, 75, and 100°C , Fig. 2(b)–(d), respectively. Only at 75°C , the sensor resistance drops again after the increase and reaches a steady state value. It is also observed that, only at 25°C , the original resistance is retained

after the increase. At the operating temperatures above 25°C , however, the increase in the sensor resistances tends to attain the steady state value, which is lower than the original sensor resistance. The decrease in the response time with increasing operating temperature is also noted in Fig. 2. The recovery of 500°C -Pt sensor is remarkably faster after the introduction of air at 760 Torr. The sensor calcined at 600°C with the Pt-sputtering exhibits sensor characteristics, Fig. 3, similar to those shown by 500°C -Pt sensor.

Typical response of In_2O_3 -doped SnO_2 sensors calcined at 500 and 600°C without Pt-sputtering, recorded for 50 ppm of hydrogen at 20 Torr air pressure, for the test-duration of approximately 24 h, is presented in Figs. 4 and 5, respectively. It is noted that the response behavior of the non-Pt-sputtered sensors calcined at 500 and 600°C is in contrary to the response behavior of 500°C -Pt and 600°C -Pt sensors. Both the non-Pt-sputtered sensors represent sluggish response kinetics during the initial test period after the introduction of H_2 . The sensor resistances, however, decrease gradually with increasing exposure time. No increase in the sensor resistance is, however, noted over the entire test-duration in the presence of H_2 . This behavior is exactly opposite to the one observed in the case of Pt-sputtered sensors, Figs. 2 and 3, where the sensor resistances increase, in the presence of H_2 , after the initial decrease. The recovery of both non-Pt-sputtered sensors is also quicker after the introduction of air at 760 Torr.

The variation in the sensitivity, response and recovery times as a function of operating temperature, for both Pt-sputtered and non-Pt-sputtered sensors calcined at 600°C , is shown in Fig. 6. It is observed that, the non-Pt-sputtered sensor exhibits higher sensitivity, at all operating temperatures, than that of the Pt-sputtered sensors. The sensitivity of both Pt-sputtered and non-Pt-sputtered sensors is observed to increase with increasing operating temperature. Further, the response time of non-Pt-sputtered sensor is noted to be higher than that of the Pt-sputtered sensor at all operating temperatures, Fig. 6(b). Moreover, the response time is observed to decrease with increasing the operating temperature. Further, the recovery time of the non-Pt-sputtered sensor is also observed to be larger than that of the Pt-sputtered sensor, Fig. 6(c). The recovery time increases first with increasing operating temperature and then decreases. The sensors calcined at 500°C , with and without Pt-sputtering exhibit similar sensing characteristics.

4. Discussion

In the present investigation, 50 ppm of H_2 is successfully sensed at lower operating temperatures (25 – 100°C) using Pt-sputtered and non-Pt-sputtered In_2O_3 -doped SnO_2 nanocrystalline thin film sensor. The mechanism of H_2 sensing using the Pt-sputtered sensor, at high ($>100^\circ\text{C}$) and low ($<100^\circ\text{C}$) operating temperatures, is schematically de-

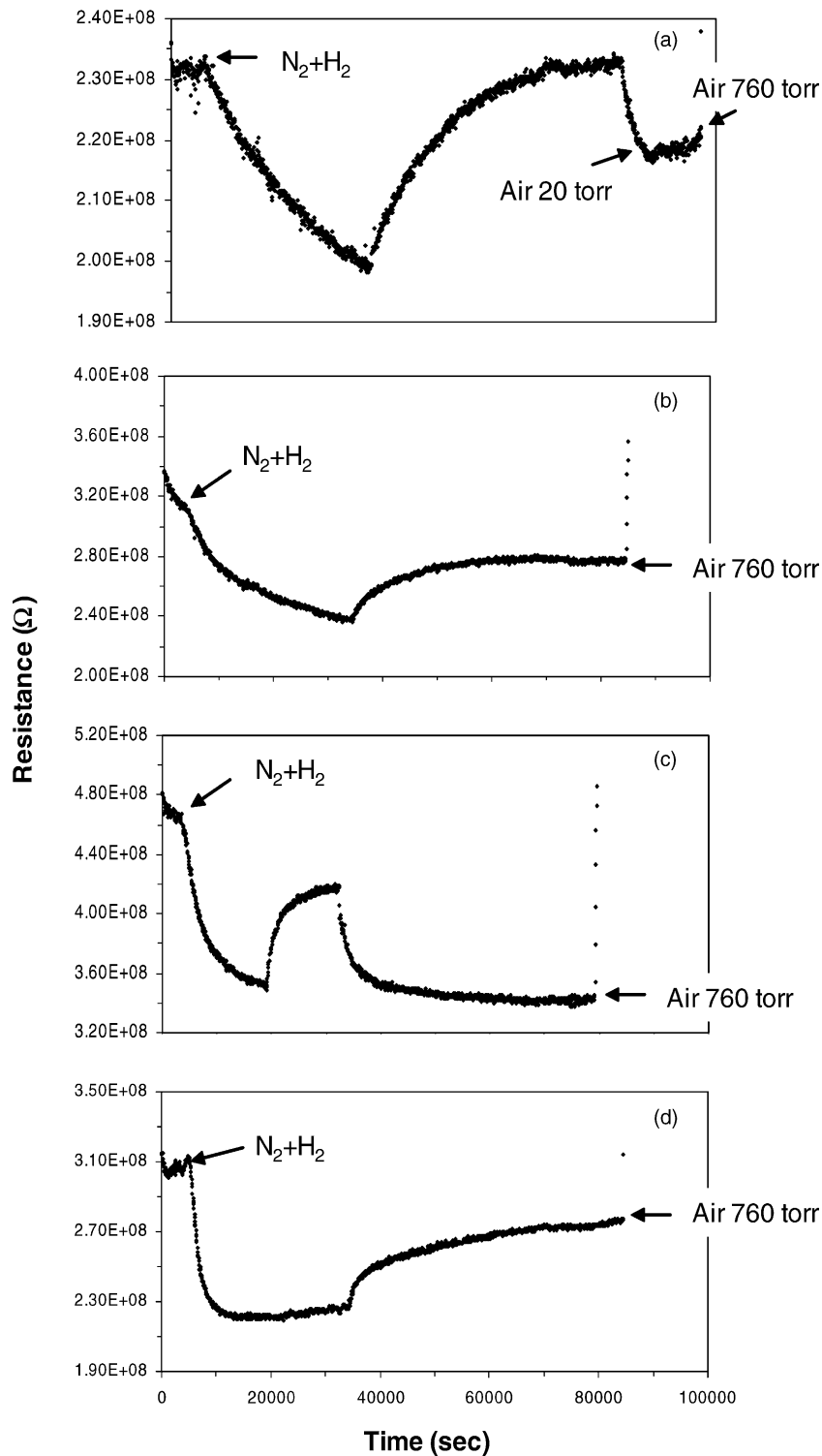


Fig. 2. Typical response of In_2O_3 -doped SnO_2 sensor to 50 ppm of H_2 . The sensor is calcined at 500°C with the Pt-catalyst and tested at different test temperatures: (a) 25°C ; (b) 50°C ; (c) 75°C ; and (d) 100°C .

scribed in Fig. 7. In the presence of Pt-catalyst on the sensor surface, the hydrogen gas splits up into the hydrogen atoms, which form protons by donating the electrons to the conduction band of nanocrystalline-doped SnO_2 film, Fig. 7(a). The electron-gain increases the film-conductivity, which is

reflected in the drop in the initial sensor-resistance, Figs. 2 and 3. The generated protons get associated with the surface-adsorbed oxygen-ions (O_2^- or O^- ions) and hop from one oxygen-ion to another. During this process, the two adjacent OH-groups may condense to form H_2O , Fig. 7(b). The

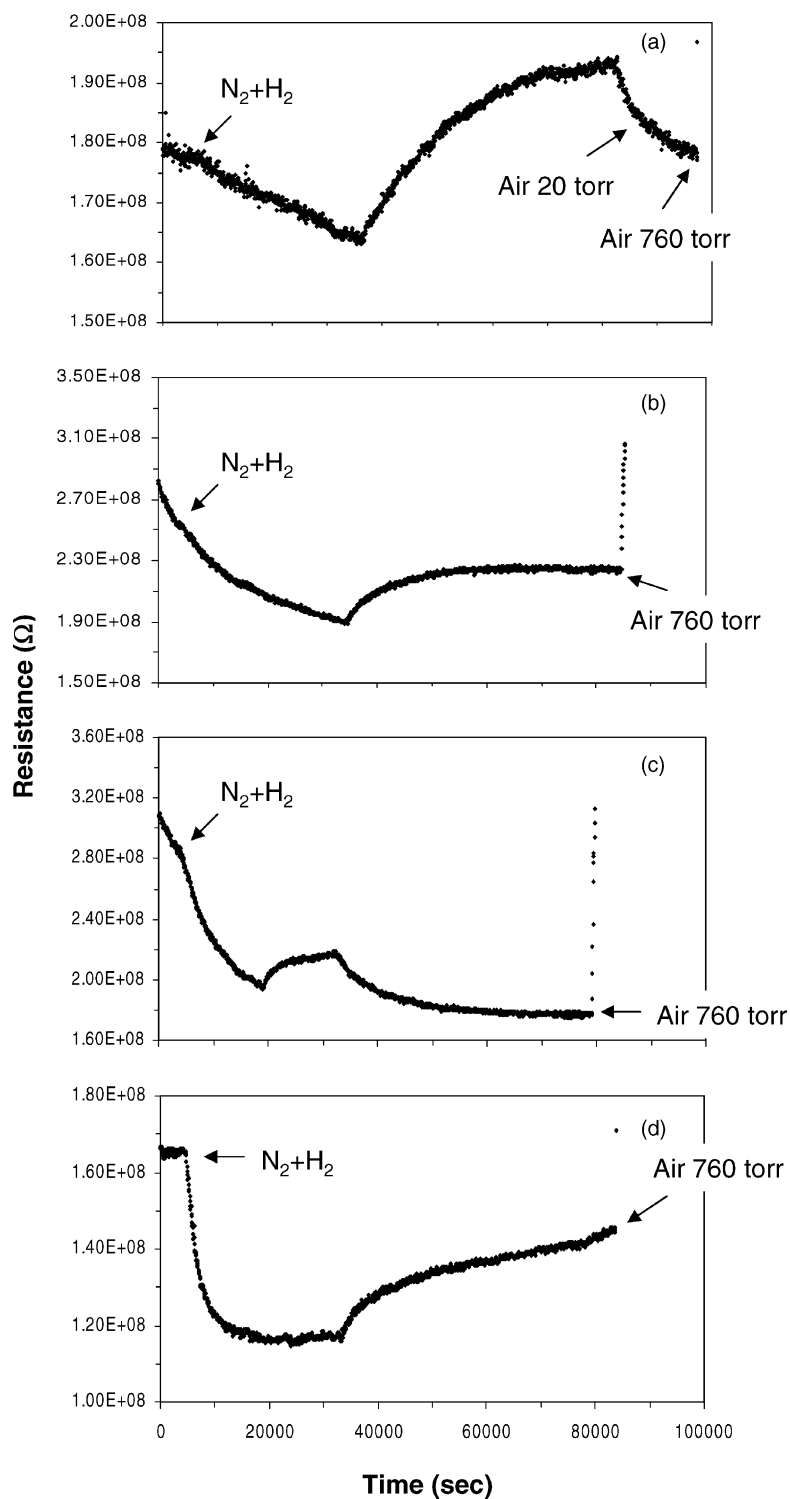


Fig. 3. Typical response of In₂O₃-doped SnO₂ sensor to 50 ppm of H₂. The sensor is calcined at 600 °C with the Pt-catalyst and tested at different test temperatures: (a) 25 °C; (b) 50 °C; (c) 75 °C; and (d) 100 °C.

overall reaction can be summarized as:



At higher operating temperatures (>100 °C), the generated H₂O molecules may get desorbed completely from the sen-

sor surface, Fig. 7(c), which may drive the reaction (1) in the forward direction. As a result, the receptor function of the nanocrystalline SnO₂ sensor is enhanced at higher operating temperatures (>100 °C), resulting in higher sensitivity values with minimum response time under these con-

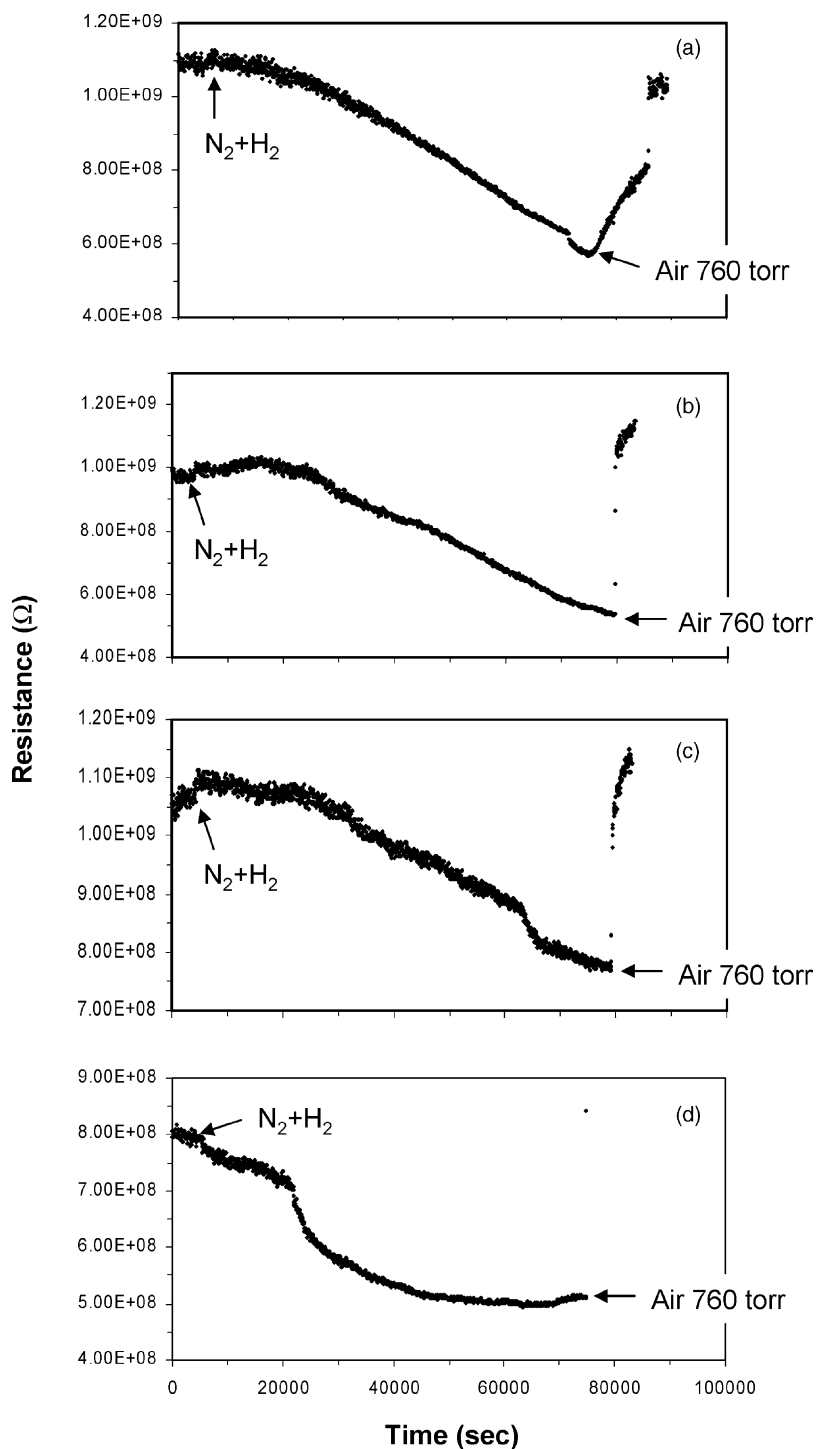


Fig. 4. Typical response of In_2O_3 -doped SnO_2 sensor to 50 ppm of H_2 . The sensor is calcined at 500°C without the Pt-catalyst and tested at different test temperatures: (a) 25°C ; (b) 50°C ; (c) 75°C ; and (d) 100°C .

ditions [7,8]. Moreover, at higher operating temperatures ($>100^{\circ}\text{C}$), the H_2 sensitivity is often reported to be higher for the sensor with the Pt-catalyst than that for the sensor without the Pt-catalyst [10]. The present sensors, when tested at lower operating temperatures ($<100^{\circ}\text{C}$) for the short test-duration (30 min), exhibit higher H_2 sensitivity in the presence of Pt-surface-catalyst, which is in consonance

with the behavior reported at higher operating temperatures ($>100^{\circ}\text{C}$).

However, the present sensors, when tested at lower operating temperatures ($<100^{\circ}\text{C}$) for long test-duration (24 h) display a reverse trend in the sensitivity values. Under this condition, at lower operating temperatures ($<100^{\circ}\text{C}$), the hydrogen sensitivity of the non-Pt-sputtered sensors is ob-

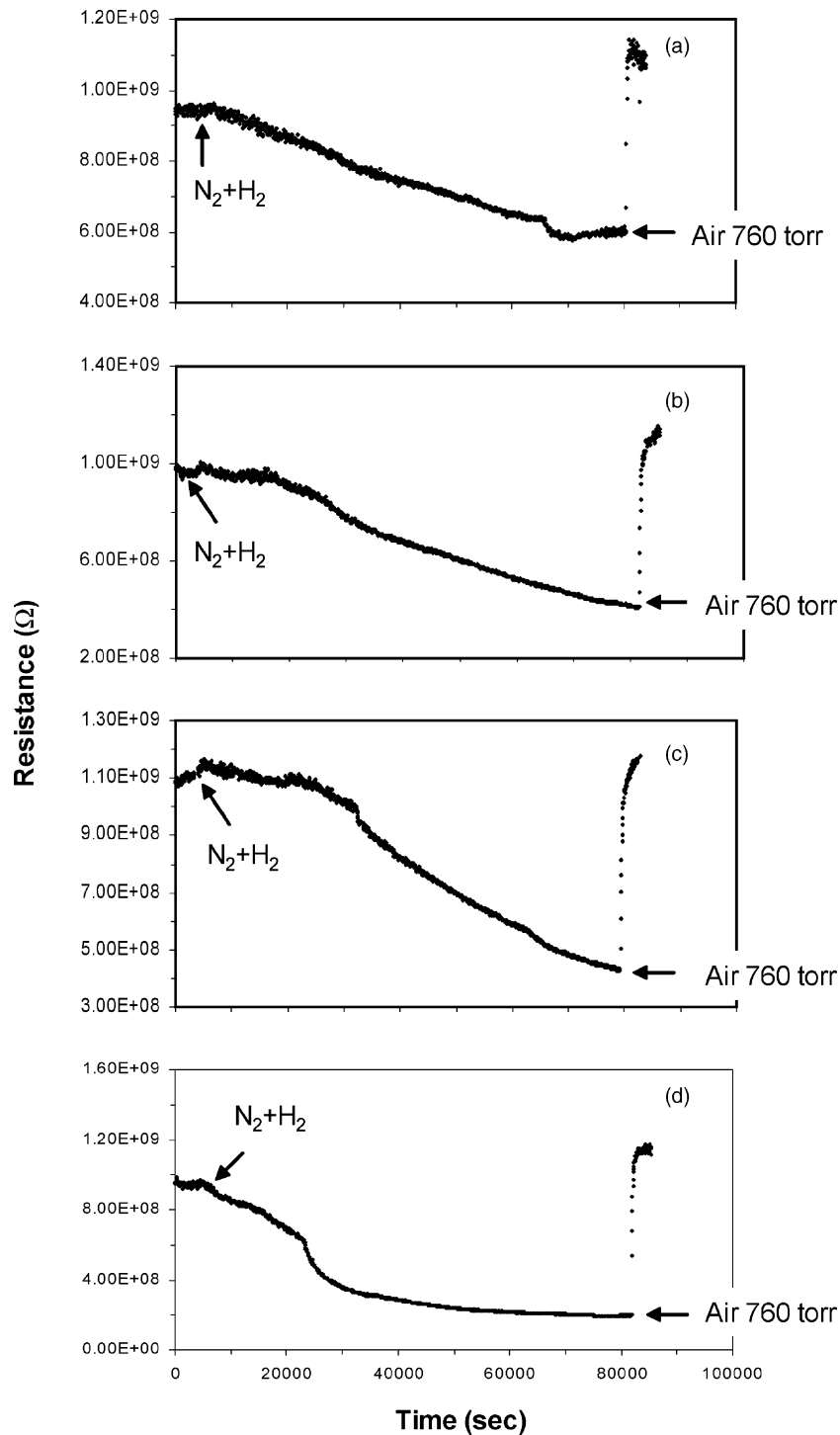


Fig. 5. Typical response of In_2O_3 -doped SnO_2 sensor to 50 ppm of H_2 . The sensor is calcined at 600°C without the Pt-catalyst and tested at different test temperatures: (a) 25°C ; (b) 50°C ; (c) 75°C ; and (d) 100°C .

served to be higher than that of the Pt-sputtered sensors, Fig. 6. Thus, the Pt-catalyst is observed to reduce the H_2 sensitivity for long test-duration (24 h) at lower operating temperatures ($<100^\circ\text{C}$). This type of sensor behavior, at lower operating temperatures, has not been reported in the literature, and hence, draws further attention.

The possible mechanism associated with an “inverse-catalyst-effect” (typically observed here at lower operating temperatures ($<100^\circ\text{C}$)) is schematically described in the Fig. 7(d) and (e). The H_2O molecules generated as a result of the condensation of adjacent OH-groups, 7(b), are not desorbed from the sensor surface at lower oper-

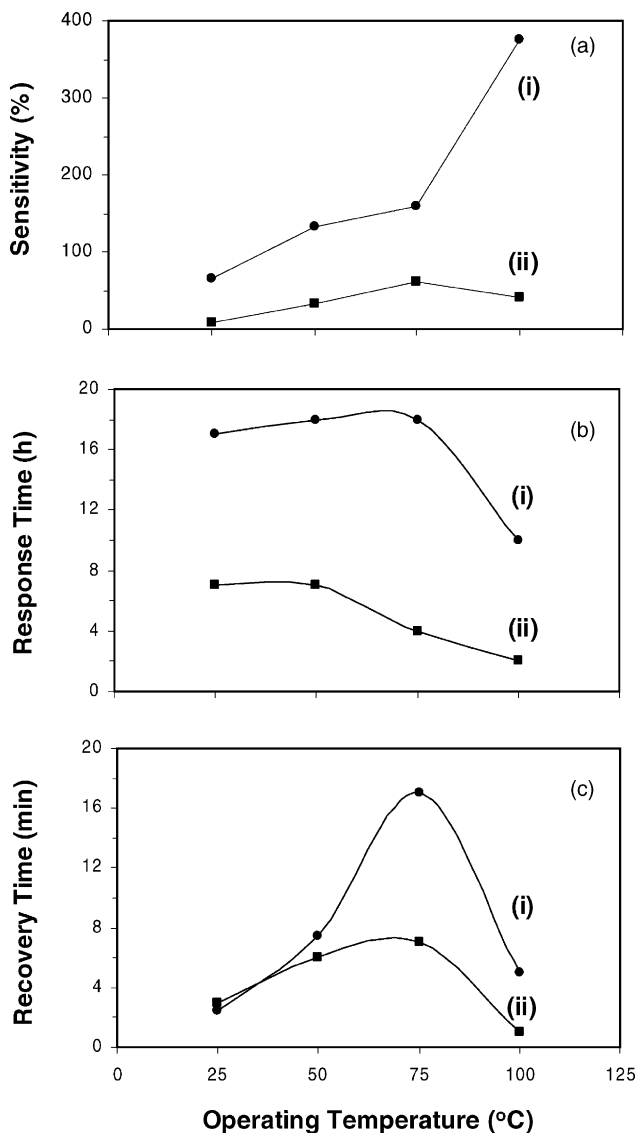


Fig. 6. Variation in the sensitivity (a); the response (b); and the recovery time (c) of In₂O₃-doped SnO₂ sensor to 50 ppm of H₂, as a function of operating temperature. The sensor is calcined at 600 °C without (i) and with (ii) the Pt-catalyst.

ating temperatures (<100 °C), Fig. 7(d). As a result, the surface concentration of H₂O molecules increases gradually with the initial drop in the sensor resistance after the introduction of H₂. In the presence of Pt-catalyst, the accumulation of high concentration surface-adsorbed H₂O molecules, drive the reaction (1) in the reverse direction as:



The reaction (2) is termed here as an “inverse-catalyst-effect”. In this process, the surface-adsorbed H₂O molecules pick-up the electrons from the conduction band of SnO₂, Fig. 7(d), thus evolving the H₂ gas and producing surface-adsorbed O⁻ ions, Fig. 7(e). The electron-loss results in the decrease in the film-conductance, which is reflected in

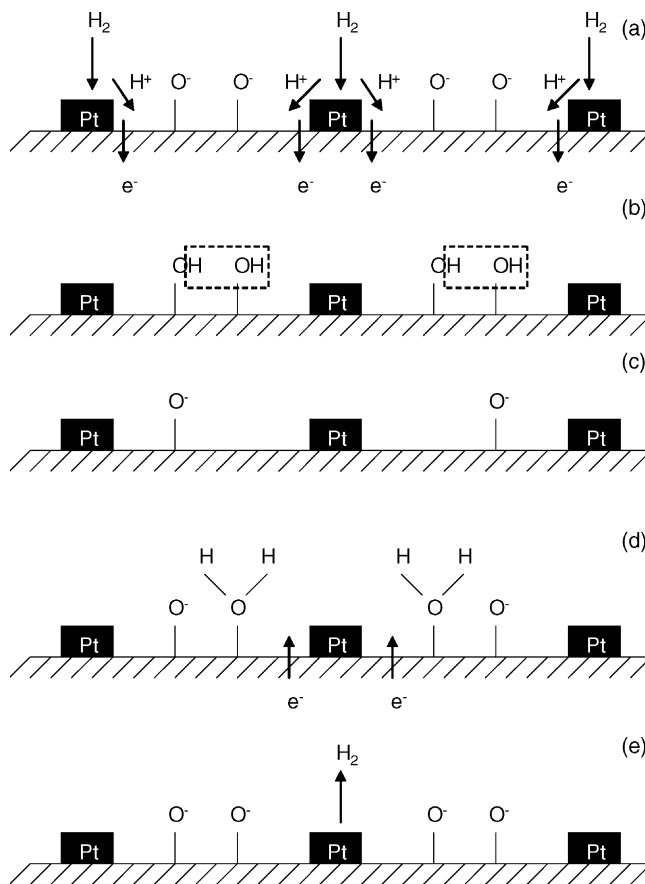


Fig. 7. Schematic representation of mechanism of H₂ sensing using the nanocrystalline In₂O₃-doped SnO₂ sensor with the Pt-catalyst, at higher operating temperatures (>100 °C) ((a)–(c)) and at lower operating temperatures ((a) and (b), (d) and (e)).

the rise in the sensor-resistance, Figs. 2 and 3. The increase in the sensor resistance via reaction (2) should reduce the surface-adsorbed concentration of H₂O molecules. Hence, after reaching the saturation resistance values, the sensor resistance in the presence of H₂ must reduce again. This type of behavior is indicated by the Pt-sputtered sensors, calcined at 500 and 600 °C, when tested at 25 °C, Figs. 2(a) and 3(a), respectively. This “inverse-catalyst-effect” is, however, not observed in the case of non-Pt-sputtered sensors, Figs. 4 and 5, which show only a gradual decrease in the sensor resistance over the entire test-duration. An “inverse-catalyst-effect” is, thus, observed to reduce the total drop in the sensor-resistance for the Pt-sputtered sensors relative to that in the case of non-Pt-sputtered ones.

The lower sensitivity values observed in the present investigation, for the Pt-sputtered sensors relative to those of non-Pt-sputtered ones, Fig. 6(a), are hence, attributed to an “inverse-catalyst-effect”. Moreover, the higher response and recovery times observed for the non-Pt-sputtered sensors relative to those of Pt-sputtered ones are attributed to their high sensitivity values than those of the latter ones, which indicate the consumption of large number of surface-adsorbed oxygen ions (O₂⁻ or O⁻ ions) by H₂. These

consumed surface-adsorbed oxygen-ions (O_2^- or O^- ions) must be re-adsorbed again in large concentration to retain the original sensor-resistance after the introduction of air. This results in higher response and recovery times when the sensitivity values are higher.

It is to be noted that, an “inverse-catalyst-effect” discussed above may not be unique to the In_2O_3 -doped SnO_2 system. It may even be observed with undoped- SnO_2 as well as for SnO_2 doped with other oxides, and even with other n-type semiconducting oxides, such as ZnO and TiO_2 . Moreover, the threshold temperature (the temperature below which an “inverse-catalyst-effect” is observed), which is greater than $100^\circ C$ for the present In_2O_3 -doped SnO_2 sensor, may be a function of different sensor-test parameters such as partial pressure of oxygen and water vapor (humidity level) within the chamber, the H_2 gas concentration, the surface characteristics of the sensor, and the nature of the catalyst used. However, such a study is beyond the scope of the present analysis; but it would be reported in the near future.

5. Conclusions

- (1) H_2 gas (50 ppm) is successfully sensed at lower operating temperatures (25 – $100^\circ C$) using the nanocrystalline In_2O_3 -doped SnO_2 thin film sensor, with and without the use of Pt-catalyst.
- (2) At lower operating temperatures (25 – $100^\circ C$), for the short test-duration (30 min), the Pt-catalyst enhances the sensitivity of the sensor relative to that of the non-Pt-sputtered ones. However, for the long test-duration (24 h), at lower operating temperatures (25 – $100^\circ C$), an “inverse-catalyst-effect” is observed, which plays a major role in reducing the sensitivity of the Pt-sputtered sensors relative to that of the non-Pt-sputtered ones.
- (3) An “inverse-catalyst-effect” appears to be a characteristic feature of nanocrystalline In_2O_3 -doped SnO_2 thin film sensor, at lower operating temperatures (25 – $100^\circ C$) and for long test-duration, in the presence of Pt-catalyst only.

Acknowledgements

Authors thank NSF CTS 0350572 and NASA Glenn for funding this sensor research.

References

- [1] S.R. Morrison, Semiconductor gas sensors, *Sens. Actuators B* 2 (1982) 329–341.
- [2] S. Seal, S. Shukla, Nanocrystalline SnO gas sensors in view of surface reactions and modifications, *JOM* 54 (9) (2002) 35–38, 60.
- [3] S. Shukla, S. Seal, Room temperature hydrogen gas sensitivity of pure tin oxide, *J. Nanosci. Nanotech.* 4 (2004) 125–129.
- [4] C. Xu, J. Tamaki, N. Miura, N. Yamazoe, Grain size effects on gas sensitivity of porous SnO_2 -based elements, *Sens. Actuators B* 3 (1991) 147–155.
- [5] F. Lu, Y. Liu, M. Dong, X. Wang, Nanosized tin oxide as the novel material with simultaneous detection towards CO , H_2 , and CH_4 , *Sens. Actuators B* 66 (2000) 225–227.
- [6] S.-S. Park, J.D. Mackenzie, Thickness and microstructure effects on alcohol sensing of tin oxide thin films, *Thin Solid Films* 274 (1996) 154–159.
- [7] G. Sakai, N.S. Baik, N. Miura, N. Yamazoe, Gas sensing properties of tin oxide thin films fabricated from hydrothermally treated nanoparticles: dependence of CO and H_2 response on film thickness, *Sens. Actuators B* 77 (2001) 116–121.
- [8] N.S. Baik, G. Sakai, N. Miura, N. Yamazoe, Hydrothermally treated sol solution of tin oxide for thin film gas sensor, *Sens. Actuators B* 63 (2000) 74–79.
- [9] S. Matsushima, T. Maekawa, J. Tamaki, N. Miura, N. Yamazoe, New methods for supporting palladium on a tin oxide gas sensor, *Sens. Actuators B* 9 (1992) 71–78.
- [10] A. Dieguez, A. Vila, A. Cabot, A.R. Rodriguez, J.R. Morante, J. Kappler, N. Barsan, U. Weimar, W. Gopel, *Sens. Actuators B* 68 (2000) 94–99.
- [11] A. Cabot, A. Dieguez, A.R. Rodriguez, J.R. Morante, N. Barsan, Influence of the catalytic introduction procedure on the nano- SnO_2 gas sensor performances: where and how stay the catalytic atoms? *Sens. Actuators B* 79 (2001) 98–106.
- [12] A. Cabot, A. Vila, J.R. Morante, Analysis of catalytic activity and electrical characteristics of different modified SnO_2 layers for gas sensors, *Sens. Actuators B* 84 (2002) 12–20.
- [13] S. Shukla, S. Patil, S.C. Kuiry, Z. Rahman, T. Du, L. Ludwig, C. Parish, S. Seal, Synthesis and characterization of sol-gel derived nanocrystalline tin oxide thin film as hydrogen sensor, *Sens. Actuators B* 96 (2003) 343–353.